Constrained observability techniques for structural system identification using modal analysis

Peng, T.; Nogal, M.; Casas, J. R.; Lozano-Galant, J. A.; Turmo, J.

Important note
To cite this publication, please use the final published version (if applicable).
Please check the document version above.

Constrained observability techniques for structural system identification using modal analysis

T. Peng [a], M. Nogal [b], J.R. Casas [a], J.A. Lozano-Galant [c], J. Turmo [a], *

[a] Department of Civil and Environmental Engineering, Universitat Politècnica de Catalunya, Barcelona, 08034, Spain
[b] Dept. of Materials, Mechanics, Management & Design, Faculty of Civil Engineering and Geosciences, Delft University of Technology, Netherlands
[c] Department of Civil Engineering, University of Castilla—La Mancha, Ciudad Real, 13071, Spain

ARTICLE INFO

ABSTRACT

The characteristics of civil structures inevitably suffer a certain level of damage during its lifetime and cheap, non-destructive and reliable methods to assess their correct performance are of high importance. Structural System Identification (SSI) using measured response is the way to fine why performance is not correct and identify where the problems can be found. Different methods of SSI exist, both using static and vibration experimental data. However, using these methods is not always possible to decide if available measurements are sufficient to uniquely obtain the unknown. A (SSI) method that uses constrained observability method (COM) has already been developed based on the information provided by the monitoring of static non-destructive tests - using deflections and rotations under a known loading case. The method assures that all observable variables can be obtained with the available measured data. In the present paper, the problem of determining the actual characteristics of the members of a structure such as axial stiffness, flexural stiffness and mass using vibration data is analyzed. Subsets of natural frequencies and/or modal shapes are used. To give a better understanding of the proposed method and to demonstrate its potential applicability, several examples of growing complexity are analyzed, and the results show how constrained observability techniques might be efficiently used for the dynamic identification of structural systems using dynamic data. These lead to significant conclusions regarding the functioning of an SSI method based on dynamic behavior.

© 2020 Elsevier Ltd. All rights reserved.

1. Introduction

The up-dated knowledge of the integrity of in-service structures through its lifetime is a very important objective for owners, end-users and both, construction and maintenance teams, to whom this information might help in decision making [1−3].

Simplified Finite Element Models (FEMs) are often used to simulate the response of civil structures [4]. When this structural response is modeled through computer simulations, mechanical and geometrical properties of the structural

---

* Corresponding author.
  E-mail addresses: tian.peng@upc.edu (T. Peng), M.Nogal@tudelft.nl (M. Nogal), joan.ramon.casas@upc.edu (J.R. Casas), JoseAntonio.Lozano@uclm.es (J.A. Lozano-Galant), jose.turmo@upc.edu (J. Turmo).

elements, such as the Young's modulus and the cross-section area are assumed to be known. Nevertheless, in most of the cases, the actual characteristics are unknown due to damage and uncertainties in the construction methods or stress state. System identification is the process of developing or improving a mathematical model of a physical system using experimental data to describe the input, output or response, and noise relationship [5]. The range of possible uses of system identification is wide. When performed in order to model a structural system, system identification allows the identification of structural parameters, such as stiffness, mass or stress and strain [6,7].

Structural System Identification (SSI) methods can be classified according to the relationship between inputs and outputs used to calibrate the model. On the one hand, non-parametric methods link outputs and inputs creating a mathematical model to characterize the system. Hence, the established relationship has no explicit physical meaning. Examples of non-parametric SSI methods might be found in Refs. [8–10]. On the other hand, parametric methods relate inputs to outputs on the basis of an actual physical meaning; due to this physical basis, this type of methods drive to a better understanding of the problem and of the sensitivity to certain parameters. Examples of these methods might be found in Refs. [11,12].

Besides the non-parametric/parametric classification, SSI might be classified depending on the nature of the excitation test used for the calibration; this is, dynamic and static ones, according to whether or not they engage inertial effects. Examples of different techniques involving static identification can be found in Refs. [13,14]. On the other hand, examples of dynamic identification methods can be found in Refs. [15–18]. There have also been attempts to combine dynamic and static data in the SSI [13,19,20].

Particularly, the observability method (OM) has recently been implemented as a SSI method in the static scenario [7]. The observability analysis lie its basis on the problem of identifying if a set of available measurements is sufficient to uniquely estimate the state of a system or of a part of it. The application of this technique has the advantage of providing, for the first time in the literature, parametric equations of the estimates. This mathematical approach has been used in other fields such as hydraulics [21], electrical and power networks [22,23] or transportation [24,25]. In addition, Lei [26] proposed the constrained observability method (COM) to overcome the deficiency of SSI by OM, which can prevent cutting off the observability tree due to the improper selection of measurement sets. However, there are researchers [27] that argue that from a practical point of view, estimation of parameters from static response is less appealing than doing it from modal or dynamic response. This is so because it is much easier to dynamically excite a large structure than statically, especially in large scale structures. Moreover, it is easier to measure accelerations than displacements because of the simplicity of establishing an inertial reference frame for measuring accelerations [27]. Hence, within the framework of observability, the problem of dynamic identification from vibration modes and frequencies can be also addressed, with a mathematical approach similar to the problem of static identification [28]. However, the observability method (OM) [29] has great limitations for complex structure and might not be able to detect any parameter.

Therefore, the aim of this paper is to propose a new constrained dynamic SSI methodology; namely, a technique that allows the identification of a subset of characteristics of a structure, such as axial or flexural stiffnesses that might be uniquely defined when a subset of natural frequencies and modal shapes is obtained from an experimental modal analysis. Two examples in Refs. [30,31] and Ref. [32] are used as a proof of concept of the dynamic COM proposed in this paper.

This paper is organized as follows. In Section 2, the constrained observability technique is presented on the basis of the formulation of the static SSI approach. In Section 3, the application of constrained observability techniques to the dynamic eigenvalue equation is described. Section 4 includes the algorithms of the dynamic constrained observability technique. A numerical example of application based on the simple frame used in Ref. [29], is used to illustrate the functioning of COM step by step, and the results from OM and COM are compared, showing the advantages of COM over OM also in the dynamic case. After that, two examples presented in the literature are employed to test the feasibility and reliability of the method when experimental data is used. Section 5 presents a large case, a multiple-story building, in order to show the applicability of the method in real structures. Finally, in Section 6, some conclusions are drawn.

2. SSI by constrained observability method: static approach

It is said that a subset of variables is observable when the system of equations derived from a set of experimental measurements implies a unique solution for this subset [3], even though the remaining variables remain undetermined. When the system is observable, it might be relevant to identify critical measurements; this is, those measurements that, if unknown, render the state of the system unobservable. Conversely, if the system is unobservable, it is relevant to identify observable islands; this is, those areas of the system whose respective states can be estimated. It is also important to identify the minimum set of additional measurements that renders the whole system observable. Therefore, observability analysis is the previous step to the identification of the system. It addresses the question of stating whether we have enough measurements to estimate the state of a system. The static approach of the SSI by OM lies its basis on the stiffness matrix method. It will be briefly introduced as it may be interesting to the reader for the sake of comparison with the dynamic observability.

The equations corresponding to this method are written in terms of nodal forces and displacements. For a certain structure, the following matrix equation can be written:

$$\mathbf{K}^{(3N_N \times 3N_N)} \boldsymbol{\delta}^{(3N_N \times 1)} = \mathbf{f}^{(3N_N \times 1)} \tag{1}$$

where **K** stands for the stiffness matrix, δ for the vector of displacements and **f** for the vector of forces; the sizes of the matrices are indicated by its superscripts, in which N_N denotes the number of nodes. To solve this system of equations, where unknowns appear in **K** (bending and axial stiffnesses); δ(displacements) and **f**(reactions); once the boundary conditions and applied forces at nodes are introduced in Eq. (1), the terms of **K** and δ can be rearranged as shown in Eq. (2), by extracting the unknown bending or axial stiffness from **K** to and removing the measured variables from δ, in such a way that K^* is a matrix of known coefficients and δ^* is a vector of knowns and unknowns, either bending or axial stiffness, unknown displacements or a product of both.

The subset δ_1^* of δ^* and the subset f_1^* of $\mathbf{f}^*$ are known, and the remaining subsets δ_0^* of δ^* and a subset f_0^* of $\mathbf{f}^*$ are not.

$$\mathbf{K}^*\delta^* = \begin{bmatrix} K_{00}^{*pxr} & K_{01}^{*pxs} \\ K_{10}^{*qxr} & K_{11}^{*qxs} \end{bmatrix} \begin{Bmatrix} \delta_0^{*rx1} \\ \delta_1^{*sx1} \end{Bmatrix} = \begin{Bmatrix} f_0^{*px1} \\ f_1^{*qx1} \end{Bmatrix} = \mathbf{f}^* \tag{2}$$

K_{00}^{*pxr}, K_{01}^{*pxs}, K_{10}^{*qxr}, K_{11}^{*qxs}, are the partitioned matrices of $\mathbf{K}^*$ and δ_0^{*rx1}, δ_1^{*sx1}, f_0^{*px1}, f_1^{*qx1} are the partitioned vectors of δ^* and $\mathbf{f}^*$ respectively. The dimensions of each of the elements are given by their superscripts.

In order to apply the OM, it is necessary to join together all the known variables in one side to form a vector **D** of known parameters and all the unknowns to the other side, forming a vector **z** of unknown parameters; this is done by rearranging the system in an equivalent form, which in this case yields into:

$$\mathbf{Bz} = \begin{bmatrix} K_{10}^{qxr} & 0 \\ K_{00}^{pxr} & -I^{pxq} \end{bmatrix} \begin{Bmatrix} \delta_0^{rx1} \\ f_0^{px1} \end{Bmatrix} = \left\{ f_1^{qx1} - K_{11}^{qxs}\delta_1^{sx1} - K_{01}^{pxs}\delta_1^{sx1} \right\} = \mathbf{D} \tag{3}$$

In Eq. (3), taking the product of unknowns in **z** as a new single variable, then $\mathbf{Bz} = \mathbf{D}$ is a system of linear equations and its general solution can be written in terms of the particular solution $\mathbf{z}_p$, and the homogeneous one, $\mathbf{z}_{nh}$, which will correspond to the case $\mathbf{Bz} = 0$. Therefore, $\mathbf{z}_p + \mathbf{z}_{nh}$ will also be a solution of the system of equations. This general solution is given by:

$$\mathbf{z} = \begin{Bmatrix} \delta_{00}^{rx1} \\ f_{00}^{px1} \end{Bmatrix} + [V]\{\rho\} \tag{4}$$

where $\begin{Bmatrix} \delta_{00}^{rx1} \\ f_{00}^{px1} \end{Bmatrix}$ is the particular solution of the system and $[V]\{\rho\}$ is the homogeneous one and represents a generic vector in the null space. In this vector, $[V]$ is a basis of the space and $\{\rho\}$ are arbitrary real values that represent the coefficients of all possible linear combinations. For the system of equations to have a unique solution vector, $[V]$ has to either be null or have some null rows. However, even if the system of equations does not have a unique solution, any unknown associated with a null row in the null space $[V]$ is observable. In this case, the general solution equals the particular one and it can be computed by calculating the pseudo inverse of matrix **B**. If there are observed parameters, the input is updated by incorporating observed variables and the previous procedure repeated until no new variables are observable. If some variables remain non-observed, the equation of the last recursive step is recorded and denoted as $\mathbf{B}_{om}\mathbf{z}_{om} = \mathbf{D}_{om}$. Here, $\mathbf{B}_{om}$, $\mathbf{z}_{om}$ and $\mathbf{D}_{om}$ are the coefficient matrix, vector of unknowns and constant vector from the last recursive step by OM, respectively.

However, it should be noted that in static SSI by OM, the vector **z** in Eq. (3) might contain two types of unknowns: (a) monomials of degree one, for example, axial and flexural stiffness, horizontal and vertical displacements, and the rotations, $\{EA_j, EI_j, u_{ik}, v_{ik}, w_{ik}\}$, and (b) monomials of degree two, for example,$\{ EA_j u_{ik}, EI_j v_{ik}, EI_j w_{ik}\}$ and they are all regarded as simple variables in **z**. In fact, there is a relation between some monomials of degree one $\{EA_j, EI_j, u_{ik}, v_{ik}, w_{ik}\}$ and monomials of degree two $\{ EA_j u_{ik}, EI_j v_{ik}, EI_j w_{ik}\}$, that is, $EA_j u_{ik} = EA_j*u_{ik}$, $EI_j v_{ik} = EI_j*v_{ik}$, $EI_j w_{ik} = EI_j*w_{ik}$. As these constrains cannot be imposed in SSI by OM because it is a linear method, the variables may not be successfully detected in some cases (i.e., it might happen that full observability is not achieved). Constrained observability method (COM) [26] is proposed to overcome the drawback of OM to continue the identification of unknown parameters by defining the residual values:

$$\varepsilon = \mathbf{B}_{om}\mathbf{z}_{om} - \mathbf{D}_{om} \tag{5}$$

The unknown variables in $\mathbf{z}_{om}$ are identified by minimizing the squared sum of the residual.

Several articles have been published regarding the SSI by OM and COM using static measurements. It is the case, for example, of [28], which studied the application of the methodology to cable-stayed bridges. Besides, in Ref. [34] a method was proposed to select the set of static measurements in order to apply SSI on bridges. The mathematical approach of these papers

was complemented by Ref. [35] by developing the numerical application of the method. Other applications of the static SSI by OM and COM include those in Refs. [26,36,37].

3. SSI by constrained observability: dynamic approach

3.1. Methodology

The application of the OM to dynamic analysis proposed in this paper is based on the dynamic equation of motion of a system with no damping and no external applied forces [37]. The equation can be expressed for a two-dimensional structure with N_N nodes, N_B boundary conditions and R vibration modes as:

$$\mathbf{K}^{[(3N_N-N_B)\times(3N_N-N_B)]}\varnothing_i^{[(3N_N-N_B)\times 1]} = \lambda_i \mathbf{M}^{[(3N_N-N_B)\times(3N_N-N_B)]}\varnothing_i^{[(3N_N-N_B)\times 1]]} \tag{6}$$
$$(i = 1, 2, 3..., R)$$

where $\mathbf{K}$ and $\mathbf{M}$ stand for the stiffness matrix and the mass matrix, respectively. Besides, $\varnothing_i$ represents the vector of modal displacements, for a 2D model with beam elements, this vector includes the deformation in the x-direction (u_{ik}), y-direction (v_{ik}) and rotation (w_{ik}) at each node k for each vibration mode i. And λ_i stand for the squared frequency for i^{th} vibration mode.

As done with the static approach [36–38], the previous Eq. (6) might be written in terms of its known and unknown parameters in modal vector, these being indicated by subscripts 1 and 0, respectively. These operations generate the modified stiffness and mass matrices $\mathbf{K}_i^*$ and $\mathbf{M}_i^*$ and the modified modal shapes $\varnothing_{Ki}^*$ and $\varnothing_{Mi}^*$ as shown in Eq. (7).

$$\mathbf{K}_i^* \varnothing_{Ki}^* = \left[K_{i,0}^{*(3N_N-N_B)\times rx} K_{i,1}^{*(3N_N-N_B)\times sx} \right] \left\{ \begin{array}{c} \varnothing_{Ki,0}^{*rx\times 1} \\ \varnothing_{Ki,1}^{*sx\times 1} \end{array} \right\}$$
$$= \left[M_{i,0}^{*(3N_N-N_B)\times mx} M_{i,1}^{*(3N_N-N_B)\times nx} \right] \left\{ \begin{array}{c} \varnothing_{Mi,0}^{*mx\times 1} \\ \varnothing_{Mi,1}^{*nx\times 1} \end{array} \right\} = \mathbf{M}_i^* \varnothing_{Mi}^* \tag{7}$$
$$(i = 1, 2, 3..., R)$$

Note that now the squared frequencies are included in the right-hand side of the equation $\mathbf{M}_i^*$ and from this step on product variables might be obtained from coupling the target unknowns with other unknowns. Examples of these product variables are $EA_j u_{ik}$, $EA_j v_{ik}$, $EI_j u_{ik}$, $EI_j v_{ik}$ and $EI_j w_{ik}$ on the left-hand side of the equation, in $\varnothing_{Ki,0}^{*rx\times 1}$, and $\lambda_i m_j u_{ik}$, $\lambda_i m_j v_{ik}$ and $\lambda_i m_j w_{ik}$ on the right-hand side, in $\varnothing_{Mi,0}^{*mx\times 1}$, where j represents the jth element and k represents k^{th} node. $\varnothing_{Mi,0}^{*mx\times 1}$ might content the simple variables u_{ik}, v_{ik}, w_{ik} once the value of $\lambda_i m_j$ is known.

As a consequence of these product variables, nonlinear parameters appear and the system of equations becomes a nonlinear one. Due to the fact that the observability technique requires linear equations in order to properly determine the observed parameters, this is solved by treating product variables as single linear variables, which linearizes the system.

The final step is to rearrange all the system in order to have all the unknowns of the system in one column vector. By doing so, it is possible to obtain the system of equations in the form Eq. (8)

$$\mathbf{B}_i \mathbf{z}_i = \left[K_{i,0}^{*(3N_N-N_B)\times rx} - M_{i,0}^{*(3N_N-N_B)\times mx} \right] \left\{ \begin{array}{c} \varnothing_{Ki,0}^{*rx\times 1} \\ \varnothing_{Mi,0}^{*mx\times 1} \end{array} \right\} = \left\{ M_{i,1}^{*(3N_N-N_B)\times nx} \varnothing_{Mi,1}^{*nx\times 1} - K_{i,1}^{*(3N_N-N_B)\times sx} \varnothing_{Ki,1}^{*sx\times 1} \right\} = \mathbf{D}_i \tag{8}$$
$$(i = 1, 2, 3..., R)$$

When multiple modal frequencies are considered together, the equation will be built by combining information of several models. For example, the first R modal information is given by $\mathbf{Bz} = \mathbf{D}$ shown as follows:

$$\mathbf{Bz} = \begin{bmatrix} B_1 & 0 & 0 & 0 \\ 0 & B_2 & 0 & 0 \\ 0 & 0 & \ddots & 0 \\ 0 & 0 & 0 & B_R \end{bmatrix} \left\{ \begin{array}{c} z_1 \\ z_2 \\ \vdots \\ z_R \end{array} \right\} = \begin{bmatrix} D_1 & 0 & 0 & 0 \\ 0 & D_2 & 0 & 0 \\ 0 & 0 & \ddots & 0 \\ 0 & 0 & 0 & D_R \end{bmatrix} = \mathbf{D} \tag{9}$$

Expression in which **B** is a matrix of constant coefficients, **D** is a fully known vector and z_i contains the full set of unknown variables. This system can be solved obtaining the solution of the coupled variables as presented in Eq. (4). Thus, the identified coupled variables (e.g., $EI_j w_{ik}$) are referred as observed variables. In other to uncouple the observed variables, e.g., $EI_j w_{ik} = EI_j^* w_{ik}$, the dynamic COM is here proposed based in a similar way as in the static case. However, in this case, the objective function is defined as:

$$J = W_\lambda \sum_{i=1}^{R} \left(\frac{\Delta \lambda_i}{\widetilde{\lambda}_i} \right)^2 + W_\varnothing \sum_{i=1}^{R} (1 - MAC_i)^2 \tag{10}$$

$$MAC_i \ (\varnothing_{mi}, \widetilde{\varnothing_{mi}}) = \frac{\left[\varnothing_{mi}^T \widetilde{\varnothing_{mi}} \right]^2}{\left(\varnothing_{mi}^T \varnothing_{mi} \right) \left(\widetilde{\varnothing_{mi}}^T \widetilde{\varnothing_{mi}} \right)} \tag{11}$$

The modal assurance criterion (MAC_i) [32] is used in Eq. (10), which consists of computing the so-called MAC values as a measure for the correspondence between the calculated mode shape $\varnothing_{mi}$, obtained from the inverse analysis using the estimated stiffnesses and areas and the measured shape $\widetilde{\varnothing_{mi}}$ as shown in Eq. (11). Besides, $\Delta \lambda_i$ are the differences between the measured, $\widetilde{\lambda}_i$, and the estimated. W_λ and $W_\varnothing$ represent the weight factors of frequencies and mode-shapes respectively. In this study, W_λ and $W_\varnothing$ are assumed to be equal [39].

The solution is obtained by minimizing Eq. (10) with the imposed constraints of the form: $EA_j u_{ik} = EA_j^* u_{ik}$, $EI_j v_{ik} = EI_j^* v_{ik}$, $EI_j w_{ik} = EI_j^* w_{ik}$ present in Eq. (9).

The proposed approach addresses the possibility of ill-conditioning by means of two actions. First, the unknowns are normalized by the a-priori best estimate, such as designer parameters (Section 4.3), which can make the condition number of coefficient matrix smaller. Second, the range of some normalized unknowns is given when the optimization process is conducted according to Eq. (10) to capture the fact that they have a physical meaning and their values cannot be either negative or extremely high (Section 5), which helps to accelerate optimization and limit value range. These two actions reduce the effect of a potential ill-conditioned equation. If the result does not make sense, then the process will be repeated with a new initial guess.

The functioning of COM will be explained step by step in Section 4 with a simple numerical example, which, additionally, fully demonstrates the excellence of COM compared to OM in the dynamic case.

4. Application of the constrained observability method to the dynamic analysis

4.1. Proposed algorithm by constrained observability

The proposed algorithm takes as inputs the topology of the structure, node connectivity and the subset of measured variables, which are the mode shapes (fully or partially known) and natural frequencies obtained from the modal analysis. On the other hand, the outputs obtained from the known data are the subset of observable variables along with their estimations.

The algorithm for the structure system identification by COM is depicted in Algorithm 1. For the sake of illustration, Section 4.2 shows its application to an academic example.

Algorithm 1 Constrained Observability Method

Input: Geometric information (*Geom*), boundary conditions (*Bound*), measured partial mode shapes and frequecies ($\varnothing_{mi,1}$, and $\lambda_{i,1}$), known structural parameters ($EI_{j,1}$, $EA_{j,1}$ and $m_{j,1}$) and number of modes to consider (*R*).
Output: Observable variables $\{EI_{,0}, EA_{,0}\}$
1: $(\mathbf{K}, \varnothing_i) \leftarrow$ BuildStiffnessMatrix (*Geom, Bound*)
2: $(\mathbf{M}, \lambda_i) \leftarrow$ BuildMassMatrix (*Geom*)
3: $(\mathbf{K}_i^*, \mathbf{M}_i^*, \varnothing_{Ki}^*, \varnothing_{Mi}^*) \leftarrow$ RearrangeMatrices ($\mathbf{K}, \mathbf{M}, \varnothing_i, \lambda_i$)
4: $([B_i], \{z_i\}, \{D_i\}) \leftarrow$ ObservabilityEquation ($\mathbf{K}_i^*, \mathbf{M}_i^*, \varnothing_{Ki}^*, \varnothing_{Mi}^*, \lambda_{i,1}, \varnothing_{mi,1}, EI_{j,1}, EA_{j,1}$)
5: $(\mathbf{B}, \mathbf{z}, \mathbf{D} \leftarrow$ CombineModalFreq ($\mathbf{B}_i, \mathbf{z}_i, \mathbf{D}_i, R$)
6: $\{Identified\} \leftarrow 1$
7: **While** $\{Identified\}$ is not empty
8 : $[V] \leftarrow$ ObtainNullSpace ($\mathbf{B}$)
9:        $\{Identified\} \leftarrow$ IdentifyObservableVariables ($[V]$)
10:        **If** $\{Identified\}$ is not empty
11:          $\{ValueIdentified\} \leftarrow$ GetParticularSolution ($\mathbf{B}, \mathbf{z}, \mathbf{D}, \{Identified\}$)
12:          $(\mathbf{B}, \mathbf{z}, \mathbf{D}) \leftarrow$ UpdateEquation ($\mathbf{B}, \mathbf{z}, \mathbf{D}, \{Identified\}, \{ValueIdentified\}$)
13:          $\{Estimated\} \leftarrow$ Collect ($\{Identified\}$)
14   **end if**

(continued on next page)

(*continued*)

Algorithm 1 Constrained Observability Method

15: **end while** %OM end
16:     ($\mathbf{B}_{om}, \mathbf{z}_{om}, \mathbf{D}_{om}$) ← ExtractEquations ($\mathbf{B}, \mathbf{z}, \mathbf{D}$)
17:     **If** $\mathbf{z}_{om}$ is not empty
18:        $\mathbf{z}^* ←$ GetHiddenUnknowns ($\mathbf{z}_{om}$)
19: ($\mathbf{B}^*, \mathbf{z}^*, \mathbf{D}_{om}$)← DefineEquations ($\mathbf{B}_{om}, \mathbf{z}_{om}, \mathbf{D}_{om}, \mathbf{z}^*$)
20:        Constraints ← GetNonlinearConstraints ($\mathbf{z}^*$)
21:        $\mathbf{z}^* ←$ Optimization ($\mathbf{B}^*, \mathbf{z}^*, \mathbf{D}_{om}$, Constraints)
22: **end** %COM end
23:     $\{EI_{,0}, EA_{,0}\} ←$ Findresult ({*Estimated*}, $\mathbf{z}^*$)

Note: Known and unknown are being indicated by subscripts 1 and 0.

4.2. Example 1 of frame by constrained observability method

In this section, the academic example presented in Fig. 1 is analyzed symbolically step by step with the objective of achieving a better understanding of the proposed methodology. The structure is composed of 2 elements and 3 nodes. One single mode of vibration is studied, although the technique can be applied to multiple vibration modes. Therefore, the size of the matrix of coefficients of the system of equations is $(3N_N - N_B) \times (3N_N - N_B)$. The structure has the vertical and horizontal displacements restrained at nodes 1 and 3, that is, $N_B = 4$. In this structure, the consistent mass matrix formulation has been used. Then, for each structural element j the mass matrix depends on the total mass of the element m_j and on its length L_j.

For the problem in Fig. 1, the axial and flexural stiffness of elements 1, EA_1, EI_1, the squared value of the first natural frequency, λ_1, the length of the elements, $L_1 = L_2 = L$, and their masses per unit length, m_1 and m_2, are assumed to be known. Besides, to show the application, three known parameters are introduced: the first natural frequency and the horizontal displacement and rotation at node 2 of the first mode shape (u_{12}, w_{12}). The known and unknowns properties are shown in Fig. 1. Thus, the input includes geometric information, boundary conditions, measured partial mode shapes and squared frequency (u_{12}, w_{12} and λ_1, known structural parameters (EA_1, EI_1 and m_1, m_2) and number of modes to consider ($R = 1$). The goal output of this analysis is EA_2 and EI_2.

If the example was experimentally analyzed, the modal frequency and the components of the vibration mode would be obtained by performing a modal analysis of measured vibrations of the real structure. In order to identify the observable variables (namely, set of variables that can be estimated on the basis of the mentioned measured data) the following steps are considered according to Algorithm 1.

Step 1. First, the characteristic equation of the system is written by building the stiffness **K** matrix of the structure, its mass matrix **M** and the modal displacements vector (line 1 and line 2). This is shown in Fig. 2.
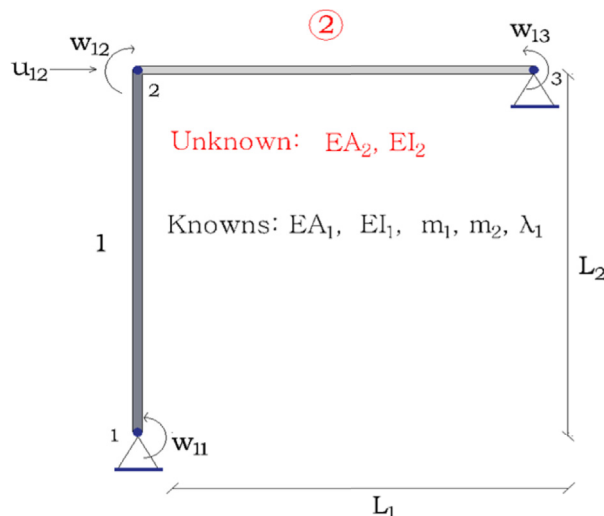

Fig. 1. Frame studied in Example 1 and degrees of freedom with positive value.

$$
\begin{bmatrix}
\frac{4EI_1}{L_1} & \frac{-6EI_1}{L_1^2} & 0 & \frac{2EI_1}{L_1} & 0 \\
\frac{-6EI_1}{L_1^2} & \frac{12EI_1}{L_1^3}+\frac{EA_2}{L_2} & 0 & \frac{-6EI_1}{L_1^2} & 0 \\
0 & 0 & \frac{EA_1}{L_1}+\frac{12EI_2}{L_2^3} & \frac{6EI_2}{L_2^2} & \frac{6EI_2}{L_2^2} \\
\frac{2EI_1}{L_1} & \frac{-6EI_1}{L_1^2} & \frac{6EI_2}{L_2^2} & \frac{4EI_1}{L_1}+\frac{4EI_2}{L_2} & \frac{2EI_2}{L_2} \\
0 & 0 & \frac{6EI_2}{L_2^2} & \frac{2EI_2}{L_2} & \frac{4EI_2}{L_2}
\end{bmatrix}
\begin{Bmatrix} w_{11} \\ u_{12} \\ v_{12} \\ w_{12} \\ w_{13} \end{Bmatrix} =
$$

$$
\lambda_1
\begin{bmatrix}
\frac{m_1 L_1^3}{105} & \frac{13m_1 L_1^2}{420} & 0 & \frac{-m_1 L_1^3}{140} & 0 \\
\frac{13m_1 L_1^2}{420} & \frac{13m_1 L_1}{35}+\frac{m_2 L_2}{3} & 0 & \frac{-11m_1 L_1^2}{210} & 0 \\
0 & 0 & \frac{m_1 L_1}{3}+\frac{13m_2 L_2}{35} & \frac{11m_2 L_2^2}{210} & \frac{-13m_2 L_2^2}{420} \\
\frac{-m_1 L_1^3}{140} & \frac{-11m_1 L_1^2}{210} & \frac{11m_2 L_2^2}{210} & \frac{m_1 L_1^3}{105}+\frac{m_2 L_2^3}{105} & \frac{-m_2 L_2^3}{140} \\
0 & 0 & \frac{-13m_2 L_2^2}{420} & \frac{-m_2 L_2^3}{140} & \frac{m_2 L_2^3}{105}
\end{bmatrix}
\begin{Bmatrix} w_{11} \\ u_{12} \\ v_{12} \\ w_{12} \\ w_{13} \end{Bmatrix}
$$

Fig. 2. Example 1. Characteristic equation of the structure in Fig. 2.

$$
\begin{bmatrix}
\frac{4}{L_1} & \frac{-6}{L_1^2} & 0 & 0 & 0 & \frac{2}{L_1} & 0 & 0 \\
\frac{-6}{L_1^2} & \frac{-12}{L_1^3} & \frac{1}{L_2} & 0 & 0 & \frac{-6}{L_1^2} & 0 & 0 \\
0 & 0 & 0 & \frac{1}{L_1} & \frac{12}{L_2^3} & 0 & \frac{6}{L_2^2} & \frac{6}{L_2^2} \\
\frac{2}{L_1} & \frac{-6}{L_1^2} & 0 & 0 & \frac{6}{L_2^2} & \frac{4}{L_1} & \frac{4}{L_2} & \frac{2}{L_2} \\
0 & 0 & 0 & 0 & \frac{6}{L_2^2} & 0 & \frac{2}{L_2} & \frac{4}{L_2}
\end{bmatrix}
\begin{Bmatrix} EI_1 w_{11} \\ EI_1 u_{12} \\ EA_2 u_{12} \\ EA_1 v_{12} \\ EI_2 v_{12} \\ EI_1 w_{12} \\ EI_2 w_{12} \\ EI_2 w_{13} \end{Bmatrix} =
$$

$$
\lambda_1
\begin{bmatrix}
\frac{L_1^3}{105} & \frac{13L_1^2}{420} & 0 & 0 & 0 & \frac{-L_1^3}{140} & 0 & 0 \\
\frac{13L_1^2}{420} & \frac{13L_1}{35} & \frac{L_2}{3} & 0 & 0 & \frac{-11L_1^2}{210} & 0 & 0 \\
0 & 0 & 0 & \frac{L_1}{3} & \frac{13L_2}{35} & 0 & \frac{11L_2^2}{210} & \frac{-13L_2^2}{420} \\
\frac{-L_1^3}{140} & \frac{-11L_1^2}{210} & 0 & 0 & \frac{11L_2^2}{210} & \frac{L_1^3}{105} & \frac{L_2^3}{105} & \frac{-L_2^3}{140} \\
0 & 0 & 0 & 0 & \frac{-13L_2^2}{420} & 0 & \frac{-L_2^3}{140} & \frac{L_2^3}{105}
\end{bmatrix}
\begin{Bmatrix} m_1 w_{11} \\ m_1 u_{12} \\ m_2 u_{12} \\ m_1 v_{12} \\ m_2 v_{12} \\ m_1 w_{12} \\ m_2 w_{12} \\ m_2 w_{13} \end{Bmatrix}
$$

Fig. 3. Example 1. Modified stiffness and mass matrices from Fig. 3.

Steps 2. To generate the modified stiffness and mass matrices, those parameters made up of several summands are separated and all the possible unknown parameters are moved to the column vectors as shown in Fig. 3 (line 3). With this, new variables appear as a result of having stiffnesses (EA_j, EI_j) coupled with modal displacements (u_{1k}, v_{1k}, w_{1k}).

Step 3. In line 4, the stiffness and mass matrices are updated by introducing the known variables. This is done by multiplying the columns associated with known variables by its corresponding values and by removing the associated factors from the vectors. Note that a new column vector appears after carrying out this step; this is a vector of independent terms, which is built by all those terms that become fully known after introducing measured variables. Since there are terms in the modified vectors of modal displacements that appear more than once, these are joined by adding together their corresponding columns resulting in $\mathbf{K}_1^*$ and $\mathbf{M}_1^*$. Besides, if there are null columns in the matrices, they can be removed together with their corresponding variable giving us vectors $\varnothing_{K1}^*$ and $\varnothing_{M1}^*$. The resulting system of equations can be seen in Fig. 4. Matrix $\mathbf{B}_i$ is assembled using matrices $\mathbf{K}_i^*$ and $\mathbf{M}_i^*$ and vector $\mathbf{z}_i$ is formed by joining all the unknown information of the system as presented in Eq. (8) as shown in Fig. 5.

Step 4. When multiple modal frequencies are considered together, the equation will be built by combining information of several models $\mathbf{B}_i\mathbf{z}_i = \mathbf{D}_i$(line 5). In this example, $R = 1$, thus $\mathbf{Bz} = \mathbf{D}$ is same as Fig. 5.

Steps 5. Afterwards, the null space $[V]$ of matrix $\mathbf{B}$ is obtained (line 8). This allows the identification of the null rows of the null space, which corresponds to the observable parameters (Fig. 6).

From the expression of z in Fig. 6, the EA_2 and w_{11} can be uniquely specified (line 9) and observable as the associated rows in $[V]$ are null and their values will not be affected by $\rho_{1.1}$, $\rho_{1.2}$ (line 11). Because it is a parametric method, the proposed technique allows the parametric expressions of the variables in this case. However, because of the complexity of these expressions they are not shown here due to space limitations.

Step 6. New variables are obtained in step 6. The unknowns obtained here in previous step, EA_2 and w_{11} are merged in to the initial inputs by OM. Therefore, the new set of variables, that is, $\{\lambda_1, w_{11}, u_{12}, EA_2$ and $w_{12}\}$ are considered as known for the next iteration to renew the $\mathbf{Bz} = \mathbf{D}$(line 12).

$$\mathbf{K}_{i,0}^{*(3N_N-N_B)\times rx} \qquad \emptyset_{Ki,0}^{*rx\times 1} \qquad \mathbf{K}_{i,1}^{*(3N_N-N_B)\times sx} \; \emptyset_{Ki,1}^{*sx\times 1}$$

$$
\begin{bmatrix}
\frac{4EI_1}{L_1} & 0 & 0 & 0 & 0 & 0 \\
\frac{-6EI_1}{L_1^2} & \frac{u_{12}}{L_2} & 0 & 0 & 0 & 0 \\
0 & 0 & \frac{EA_1}{L_1} & \frac{12}{L_2^3} & \frac{6w_{12}}{L_2^2} & \frac{6}{L_2^2} \\
\frac{2EI_1}{L_1} & 0 & 0 & \frac{6}{L_2^2} & \frac{4w_{12}}{L_2} & \frac{2}{L_2} \\
0 & 0 & 0 & \frac{6}{L_2^2} & \frac{2w_{12}}{L_2} & \frac{4}{L_2}
\end{bmatrix}
\begin{Bmatrix} w_{11} \\ EA_2 \\ v_{12} \\ EI_2 v_{12} \\ EI_2 \\ EI_2 w_{13} \end{Bmatrix}
+
\begin{Bmatrix}
\frac{2EI_1 w_{12}}{L_1}+\frac{-6EI_1 u_{12}}{L_1^2} \\
\frac{-6EI_1 w_{12}}{L_1^2}+\frac{12EI_1 u_{12}}{L_1^3} \\
0 \\
\frac{4EI_1 w_{12}}{L_1}+\frac{-6EI_1 u_{12}}{L_1^2} \\
0
\end{Bmatrix}
=
$$

$$
\lambda_1
\begin{bmatrix}
\frac{m_1 L_1^3}{105} & 0 & 0 \\
\frac{13m_1 L_1^2}{420} & 0 & 0 \\
0 & \frac{m_1 L_1}{3}+\frac{13m_2 L_2}{35} & \frac{-13m_2 L_2^2}{420} \\
\frac{-m_1 L_1^3}{140} & \frac{11m_2 L_2^2}{210} & \frac{-m_2 L_2^3}{140} \\
0 & \frac{-13m_2 L_2^2}{420} & +\frac{m_2 L_2^3}{105}
\end{bmatrix}
\begin{Bmatrix} w_{11} \\ v_{12} \\ w_{13} \end{Bmatrix}
+\lambda_1
\begin{Bmatrix}
\frac{-m_1 w_{12} L_1^3}{140}+\frac{13m_1 L_1^2 u_{12}}{420} \\
\frac{-11m_1 w_{12} L_1^2}{210}+\frac{13m_1 L_1 u_{12}}{35}+\frac{m_2 L_2 u_{12}}{3} \\
\frac{11m_2 w_{12} L_2^2}{210} \\
\frac{m_1 w_{12} L_1^3}{105}+\frac{m_2 w_{12} L_2^3}{105}+\frac{-11m_1 L_1^2 u_{12}}{210} \\
\frac{-m_2 w_{12} L_2^3}{140}
\end{Bmatrix}
$$

$$\mathbf{M}_{i,0}^{*(3N_N-N_B)\times mx} \qquad \emptyset_{Mi,0}^{*mx\times 1} \qquad \mathbf{M}_{i,1}^{*(3N_N-N_B)\times nx}\; \emptyset_{Mi,1}^{*nx\times 1}$$

Fig. 4. Example 1. Modified stiffness and mass matrices of the structure in Fig. 2 after updating them with measured variables and summing up the columns with common terms.

$$
\begin{bmatrix}
\frac{4EI_1}{L_1}-\frac{\lambda_1 m_1 L_1^3}{105} & 0 & 0 & 0 & 0 & 0 & 0 \\
\frac{-6EI_1}{L_1^2}-\frac{13\lambda_1 m_1 L_1^2}{420} & \frac{u_{12}}{L_2} & 0 & 0 & 0 & 0 & 0 \\
0 & 0 & \frac{12}{L_2^3} & \frac{EA_1}{L_1}-\frac{\lambda_1 m_1 L_1}{3}-\frac{13\lambda_1 m_2 L_2}{35} & \frac{6w_{12}}{L_2^2} & \frac{6}{L_2^2} & \frac{13\lambda_1 m_2 L_2^2}{420} \\
\frac{2EI_1}{L_1}+\frac{\lambda_1 m_1 L_1^3}{140} & 0 & \frac{6}{L_2^2} & -\frac{11\lambda_1 m_2 L_2^2}{210} & \frac{4w_{12}}{L_2} & \frac{2}{L_2} & \frac{\lambda_1 m_2 L_2^3}{140} \\
0 & 0 & \frac{6}{L_2^2} & \frac{13\lambda_1 m_2 L_2^2}{420} & \frac{2w_{12}}{L_2} & \frac{4}{L_2} & \frac{\lambda_1 m_2 L_2^3}{105}
\end{bmatrix}
\begin{Bmatrix} w_{11} \\ EA_2 \\ EI_2 v_{12} \\ v_{12} \\ EI_2 \\ EI_2 w_{13} \\ w_{13} \end{Bmatrix}
=
$$

$$
\begin{Bmatrix}
\frac{13\lambda_1 m_1 L_1^2 u_{12}}{420}+\frac{-m_1 L_1^3 w_{12}}{140}+\frac{6EI_1 u_{12}}{L_1^2}-\frac{2EI_1 w_{12}}{L_1} \\
\frac{13\lambda_1 m_1 L_1 u_{12}}{35}+\frac{\lambda_1 m_2 L_2 u_{12}}{3}+\frac{-11m_1 L_1^2 w_{12}}{210}-\frac{12EI_1 u_{12}}{L_1^3}+\frac{6EI_1 w_{12}}{L_1^2} \\
\frac{11m_2 L_2^2 w_{12}}{210} \\
\frac{-11\lambda_1 m_1 L_1^2 u_{12}}{210}+\frac{m_1 L_1^3 w_{12}}{105}+\frac{m_2 L_2^3 w_{12}}{105}+\frac{6EI_1 u_{12}}{L_1^2}-\frac{4EI_1 w_{12}}{L_1} \\
\frac{-m_2 L_2^3 w_{12}}{140}
\end{Bmatrix}
$$

Fig. 5. Example 1. System of equations in the form of Eq. (9) for the structure in Fig. 2.

Step 7. EA_2 and w_{11} are collected into the list of estimated items (line 13).

Step 8. Given that some variables were identified in the previous iteration, a next iteration starts. The null space, $[V]$ and the general solution of Fig. 7 (line 8), are given as:

$$\mathbf{z} = \mathbf{z}_p + [V]\{\rho\} = \begin{Bmatrix} w_{11} \\ EA_2 \\ EI_2 v_{12} \\ v_{12} \\ EI_2 \\ EI_2 w_{13} \\ w_{13} \end{Bmatrix}_p + \begin{Bmatrix} 0 & 0 \\ 0 & 0 \\ -L & -\dfrac{132EA_1 L^5 \lambda_1 m_2 - 44 L^7 \lambda_1^2 m_1 m_2 - 27 L^7 \lambda_1 m_2^2}{504(-60EA_1 + 20L^2\lambda_1 m_1 + 21L^2\lambda_1 m_2)} \\ 0 & \dfrac{2L^3 \lambda_1 m_2}{-60EA_1 + 20L^2\lambda_1 m_1 + 21L^2\lambda_1 m_2} \\ -1/w_{12} & -\dfrac{L^4(60EA_1\lambda_1 m_2 - 20L^2\lambda_1^2 m_1 m_2 - 11L^2\lambda_1 m_2^2)}{120 w_{12}(60EA_1 - 20L^2\lambda_1 m_1 - 21L^2\lambda_1 m_2)} \\ 1 & 0 \\ 0 & 1 \end{Bmatrix} \begin{Bmatrix} \rho_{1.1} \\ \rho_{1.2} \end{Bmatrix}$$

Fig. 6. Example 1. Solution given by the particular and the homogeneous solution.

Step9. It is obvious that no new variable is observable as no null row exists in the null space of $[V]$ (line 9). Therefore, no new yielded variable can be identified through the OM (line 10), thus, the iterative process of line 7 stops (line 14).

Steps 10. Extract the equation $\mathbf{B}_{om}\mathbf{z}_{om} = \mathbf{D}_{om}$ from OM, Fig. 7 (line 16). Only partial observability is achieved and still 3 unknowns remain, especially the stiffness EI_2. Hence, the full observability is not achieved, triggering the execution of COM (from line 17). and check if hidden unknowns exist or not (line 18). First split the complex variables $\mathbf{z}_c = \{EI_2 v_{12}, EI_2 w_{13}\}$ of $\mathbf{z}_2$ into single ones $\{EI_2, v_{12}, w_{13}\}$, which are included in single variables $\mathbf{z}_s = \{EI_2, v_{12}, w_{13}\}$. Thus $\mathbf{z}^* = \{EI_2 v_{12}, EI_2 w_{13}, EI_2, v_{12}, w_{13}\}$, $\mathbf{B}^* \mathbf{z}^* = \mathbf{B}_{om}\mathbf{z}_{om} = \mathbf{D}_{om}$ (line 19).

Steps 11. Identify the nonlinear constraints in $\mathbf{z}^*$ (line 20). Establish the constraints $EI_2 v_{12} = EI_2^* v_{12}, EI_2 w_{13} = EI_2^* w_{13}$. Then an optimization routine, is used to achieve the fully exploitation of the information in measurements with the acquired nonlinear constraints and all the parameters observed (line 21). In the optimization process, the nonlinear constraints are imposed by ensuring the equality between the coupled unknowns and the product of corresponding single unknowns. Thus, all the unknowns are obtained successfully.

$$\mathbf{Bz} = \begin{bmatrix} 0 & 0 & 0 & 0 & 0 \\ 0 & 0 & 0 & 0 & 0 \\ \dfrac{12}{L_2^3} & \dfrac{6w_{12}}{L_2^2} & \dfrac{6}{L_2^2} & \dfrac{EA_1}{L_1} - \dfrac{\lambda_1 m_1 L_1}{3} - \dfrac{13\lambda_1 m_2 L_2}{35} & \dfrac{13\lambda_1 m_2 L_2^2}{420} \\ \dfrac{6}{L_2^2} & \dfrac{4w_{12}}{L_2} & \dfrac{2}{L_2} & -\dfrac{11\lambda_1 m_2 L_2^2}{210} & \dfrac{\lambda_1 m_2 L_2^3}{140} \\ \dfrac{6}{L_2^2} & \dfrac{2w_{12}}{L_2} & \dfrac{4}{L_2} & \dfrac{13\lambda_1 m_2 L_2^2}{420} & -\dfrac{\lambda_1 m_2 L_2^3}{105} \end{bmatrix} \begin{Bmatrix} EI_2 v_{12} \\ EI_2 \\ EI_2 w_{13} \\ v_{12} \\ w_{13} \end{Bmatrix} =$$

$$\begin{Bmatrix} -\dfrac{4EI_1 w_{11}}{L_1} + \dfrac{6EI_1 u_{12}}{L_1^2} + \dfrac{\lambda_1 m_1 w_{11} L_1^3}{105} + \dfrac{13\lambda_1 m_1 u_{12} L_1^2}{420} - \dfrac{2EI_1 w_{12}}{L_1} - \dfrac{\lambda_1 m_1 L_1^3 w_{12}}{140} \\ \dfrac{6EI_1 w_{11}}{L_1^2} + \dfrac{12EI_1 u_{12}}{L_1^3} + \dfrac{13\lambda_1 m_1 w_{11} L_1^2}{420} + \dfrac{13\lambda_1 m_1 u_{12} L_1}{35} + \dfrac{\lambda_1 m_2 u_{12} L_2}{3} - \dfrac{EA_2 u_{12}}{L_2} + \dfrac{6EI_1 w_{12}}{L_1^2} - \dfrac{11\lambda_1 m_1 L_1^2 w_{12}}{210} \\ \dfrac{11\lambda_1 m_2 L_2^2}{210} \\ -\dfrac{2EI_1 w_{11}}{L_1} + \dfrac{6EI_1 u_{12}}{L_1^2} - \dfrac{\lambda_1 m_1 w_{11} L_1^3}{140} - \dfrac{11\lambda_1 m_2 L_2^2 u_{12}}{210} - \dfrac{4EI_1 w_{12}}{L_1} + \dfrac{\lambda_1 m_1 L_1^3 w_{12}}{105} - \dfrac{\lambda_1 m_2 L_2^3 w_{12}}{105} \\ -\dfrac{\lambda_1 m_2 L_2^3 w_{12}}{140} \end{Bmatrix} = \mathbf{D}$$

Fig. 7. Example 1. System of equations in the form of Eq. (9) for the structure in Fig. 2.

$$\mathbf{z}_2 = \mathbf{z}_{p2} + [V]_2\{\rho\}_2 = \begin{Bmatrix} EI_2 v_{12} \\ EI_2 \\ EI_2 w_{13} \\ v_{12} \\ w_{13} \end{Bmatrix}_p + \begin{Bmatrix} -L & \dfrac{L^5\lambda_1 m_2(44L^2\lambda_1 m_1 - 132E_1 A_1 + 27L^2\lambda_1 m_2)}{504(20L^2\lambda_1 m_1 - 60E_1 A_1 + 21L^2\lambda_1 m_2)} \\ \dfrac{1}{w_{12}} & \dfrac{L^2(11L^4\lambda_1^2 m_2^2 + 20m_1 L^4\lambda_1^2 m_2 - 60E_1 A_1 L^3\lambda_1 m_2)}{120 w_2(20L^2\lambda_1 m_1 - 60E_1 A_1 + 21L^2\lambda_1 m_2)} \\ 1 & 0 \\ 0 & \dfrac{(2L^3\lambda_1 m_2)}{20L^2\lambda_1 m_1 - 60E_1 A_1 + 21L^2\lambda_1 m_2} \\ 0 & 1 \end{Bmatrix} \begin{Bmatrix} \rho_{2.1} \\ \rho_{2.2} \end{Bmatrix}$$

Fig. 8. Example 1. Solution given by the particular and the homogeneous solution.
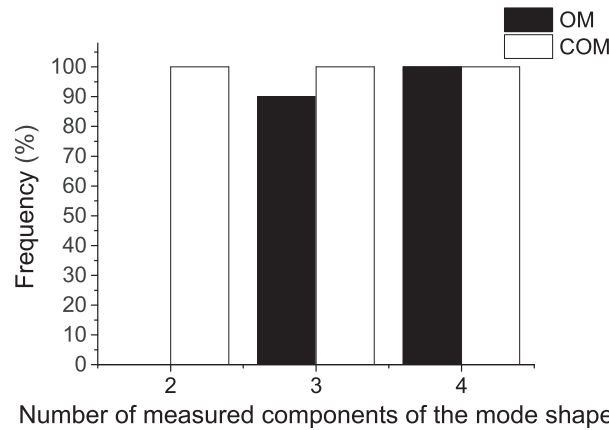
Fig. 9. Frequency of the occurrence of fully observability by OM and COM in the first mode.

As shown, just using OM (step 1 to step 10) to solve the problem, the structural parameter, EI_2, cannot be identified, and the recursive process will end at step 10. Although $\rho_{2.1}$ and $\rho_{2.2}$ in Fig. 8 play the essential role to make the establishment of constraints $EI_2v_{12} = EI_2{}^*v_{12}$, $EI_2w_{13} = EI_2{}^*w_{13}$ and to make sure the identification of EI_2v_{12}, EI_2w_{13}, EI_2, v_{12}, w_{13}, the value of $\rho_{2.1}$ and $\rho_{2.2}$ cannot be uniquely determined by OM. Hence, the main idea of COM is to introduce the nonlinear constraint relationship between the coupled unknowns and single unknowns of OM. After that, the optimization is performed to achieve fully observability by the objective function in Eq. (10).

Fig. 9 shows the comparison of fully observability obtained by OM and by COM for this simple structure. It can be seen that COM, as an extended version of OM, enhances the performance of OM. Especially, the frequency of fully observability soars from 0 to 100% when the number of measured components of the first mode shape is equal to 2. The larger the number of measured components, the larger the likelihood of fully observability, nevertheless, the restriction of the feasible number of sensors in real structures should be considered. Because the values of the mode-shapes are normalized by a reference value, considering just one single measure of each vibration mode does not provide meaningful information, therefore single measures can be ignored. Hence, COM has demonstrated great superiority when compared to OM even in this simple case with numerical and non-experimental values. Therefore, COM should be strongly recommended in the following examples where real experimental data is used.

4.3. Example 2—TWO DOF by constrained observability

In this example, taken from Ref. [30], the reliability of the proposed dynamic COM method is checked when experimental data is considered. Whereas a simple academic example was used in the previous section for the sake of illustration, this example allows the comparison of the method with existing results.

The dynamic COM is applied to identify the stiffness properties of two floors. For this, the structure is modeled by a two-DOF linear lumped mass shear building model as schematically shown in Fig. 10 a). In the modeling, the masses are treated as
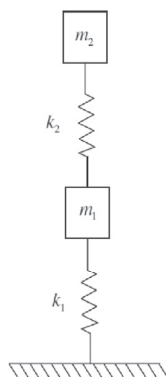
Experimental modal frequencies and mode-shapes of the two-story aluminum building model.

		Mode 1	Mode 2
Modal frequencies (Hz)		17.2	50.4
Modeshapes	1st Floor	0.48	−1.23
	2nd Floor	1.00	1.00

a)   b)

Fig. 10. (a) Two DOF lumped mass model (b) experimental modal frequencies and mode-shapes.

Table 1
Observed properties in Fig. 12.

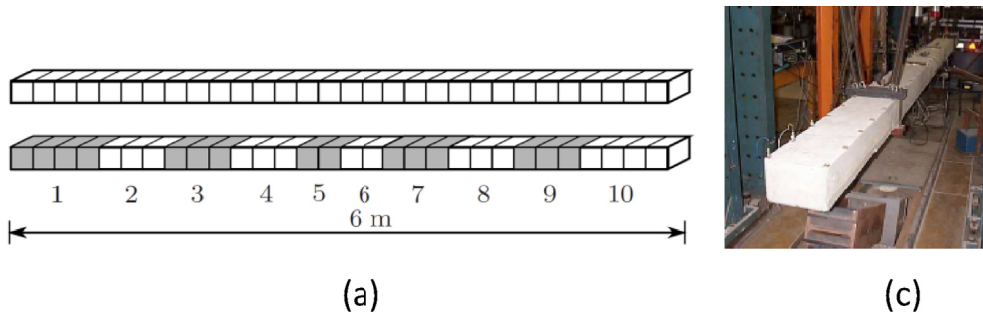| Method	Fully Observability	$x = [x_1 \ x_2]$	$\Delta f_1(\%)$	$\Delta f_2(\%)$	$MAC(\varnothing_i, \overline{\varnothing}_j)$
COM	YES	[0.5167 0.7091]	0.32	−0.42	$\begin{bmatrix} 0.976 & 0.0063 \\ 0.010 & 0.982 \end{bmatrix}$
Reference results 1	YES	[0.546 0.648]	1.384	−3.174	$\begin{bmatrix} 0.983 & 0.011 \\ 0.006 & 0.976 \end{bmatrix}$
Reference results 2	YES	[0.511 0.718]	0.025	−0.057	$\begin{bmatrix} 0.974 & 0.0057 \\ 0.011 & 0.983 \end{bmatrix}$

Fig. 11. (a) set-up of static loading (b) image of vibration testing [32].

deterministic, while the model parameters are chosen to be the two interstory stiffness of the two-story building. According to Ref. [30], the model masses were estimated from the structural drawings to be $m_1 = 3.9562$ kg and $m_2 = 4.4482$ kg. The a priori best estimate of the interstory stiffness calculated from the structural drawings is the same for both stories and equal to $k_0 = 2.3694 \times 10^5$ Nm^{-1}. The following parameterization of the two- DOF model shown in Fig. 10 is used: $k_i = x_i k_0$, $i = 1, 2$, which can avoid the ill-posed problems since the unknowns x_i were normalized by the a-priori best estimate and it can reduce the morbidity of the matrix. The purpose of the identification is to update the values of the stiffness parameters x_1 and x_2 using the measured modal data reported in Fig. 12 b).

Through the COM analysis, the results are displayed in Table 1, and compared with the two reference results [30]. Here, the measured data in Fig. 10 b) are assumed as true values.

From Table 1, the results of frequencies from COM are between Reference results 1 and 2. The total errors of frequencies and MAC of the results are calculated by the sum of squares of the difference between the obtained and the theoretical values obtaining, $E_{f-com} = 2.75 \times 10^{-5}$, $E_{MAC-com} = 1.039 \times 10^{-3}$ and $E_{f-Re2} = 3.874 \times 10^{-7}$, $E_{MAC-Re2} = 1.12 \times 10^{-3}$. Reference results 2, $x = [0.511 \ 0.718]$, fit very well the frequency properties to values as low as $E_{f-Re2} = 3.874 \times 10^{-7}$ at the expense of deteriorating significantly the fit of modal properties to the values as high $E_{MAC-Re2} = 1.12 \times 10^{-3}$ compared with the COM results. This could suggest that if the tiny sacrifice in the fit of frequencies is not of concern in the identification to preserve the accuracy of modal information, the results of COM $x = [0.5167 \ 0.7091]$ are is the most representative of this structure.

4.4. Example 3—Reinforced concrete beam by constrained observability

The dynamic COM is applied to the damage assessment of a reinforced concrete beam with a length of 6 m and dimensions as shown in Fig. 11 [32]. The transverse mode shape displacements are observed at 31 point equidistant locations along the beam, and the resulting mode shape measurements are shown with their corresponding natural frequencies in Fig. 14. Initially, all bending stiffness parameters are assumed to be equal $EI_{int} = 7.23 \times 10^6$ Nm^{-2}. The beam is divided into 10 substructures with a uniform stiffness value or Young's modulus in Fig. 11 (a). The following parameterization of the 10 bending stiffness model shown in Fig. 12 is used: $EI_i = x_i EI_{int}$, $i = 1 \sim 10$. The purpose of the identification is to update the values of the stiffness parameters $x_1 \sim x_{10}$ using the measured modal data reported in Fig. 12.

The estimated yielded by COM analysis are [1.153 1.031 0.860 0.903 0.799 0.511 0.563.

0.717 0.864]. Here, the measured data in Fig. 12 are assumed as true values, which come from the original data shown in Ref. [32]. This result gives the engineer the best approximation, as justified below, and determines the location of damage; the most serious damage is located in substructure 6 and 7. The comparison of frequencies and MAC are shown in Table 2 where these are provided with high precision. All the errors between the estimated frequencies and the experimental ones are lower
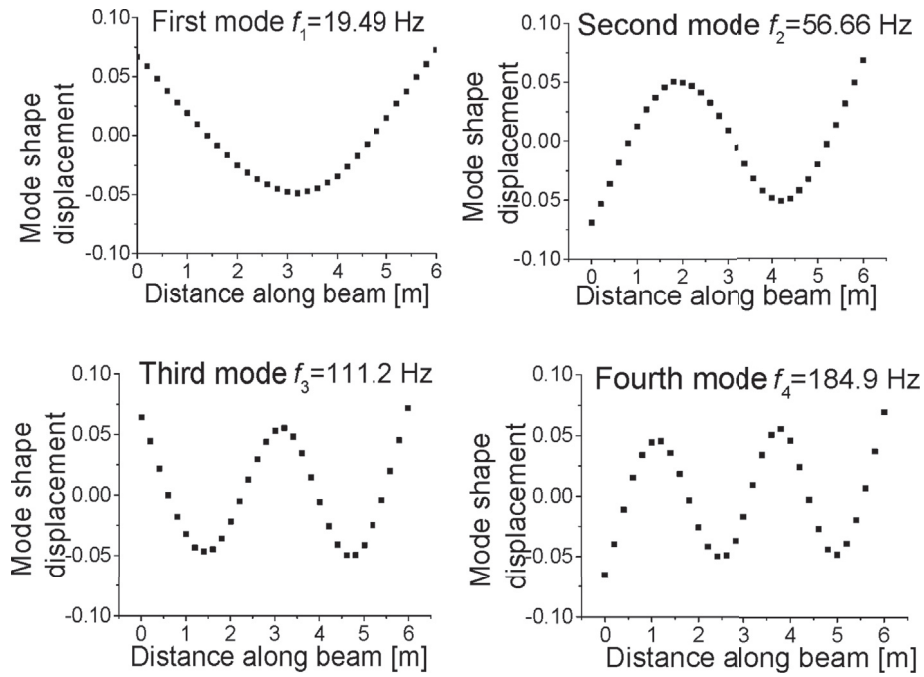
Fig. 12. The first four experimental bending mode and the corresponding frequencies.

Table 2
Observed properties in Fig. 13.

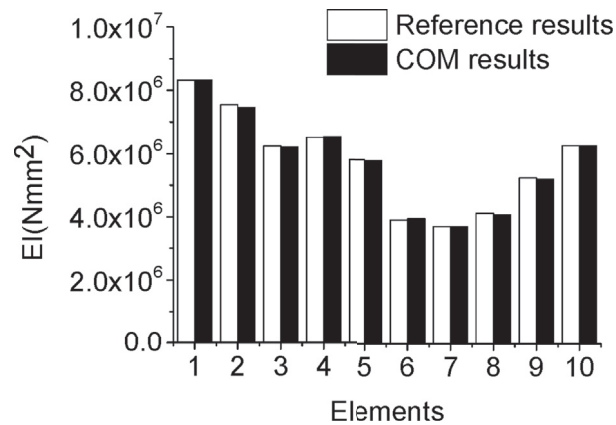| Method	Fully Observability	$x = [x_1 \sim x_{10}]$	Mode	$\Delta f(\%)$	MAC$(\varnothing_i, \overline{\varnothing}_i)$
COM	YES	[1.154 1.029 0.856	1	−1.05	0.996
		0.902 0.797 0.544	2	−0.76	0.999
		0.508 0.560 0.713	3	−0.04	0.999
		0.864]	4	1.68	0.999

Fig. 13. Bending stiffness of COM method and Reference results [32].

than 5%. This value is the maximum precision that can be expected according to the results presented in Ref. [33] for a reinforced concrete structure. In addition, MAC is very close to 1, that is to say, the estimated mode shapes fit well with the data from Fig. 12. Regarding the comparison between these estimated stiffnesses and the values from Ref. [32] and from Fig. 13, it is to highlight that the largest difference between two outcomes is 1.2%.
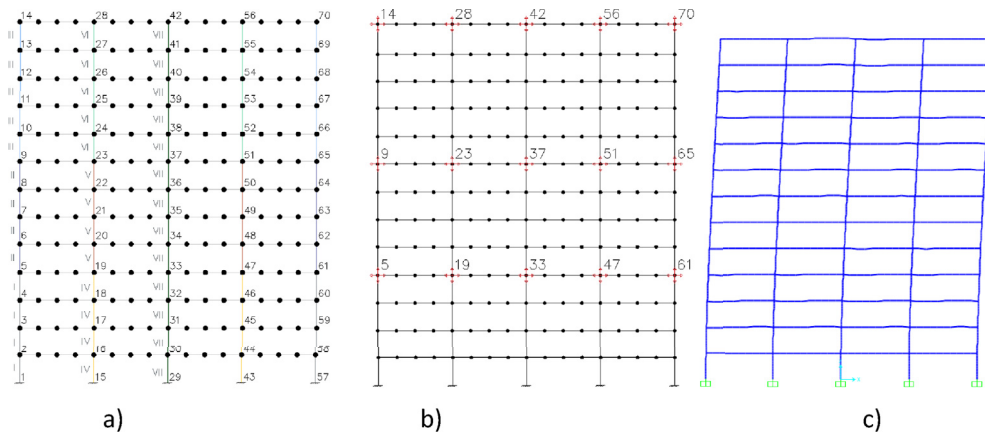
Fig. 14. Illustration of the 13-floor frame studied in Example 3. (a)The members with different characteristics are represented with different colours, (b) Sets of measurements used in the global analysis, (c) First mode shape. (For interpretation of the references to colour in this figure legend, the reader is referred to the Web version of this article.)

Table 3
Properties of the frame shown in Fig. 14.

Section	Elements	$A(m^2)$	$I(m^4)$
I : Outer Bottom Columns	1 to 4 and 53 to 56	0.563	0.026
II : Outer Intermediate Columns	5 to 8 and 57 to 60	0.360	0.011
III : OuterUpper Columns	9 to 13 and 61 to 65	0.250	0.005
IV : Interior Bottom Columns	14 to 17and 40 to 43	0.360	0.011
V : Interior Intermediate Columns	18 to 21and 44 to 47	0.250	0.011
VI : Interior Upper Columns	22 to 26 and 48 to 52	0.160	0.002
VII : Central Core	27 to 39	1.800	5.400
VIII : Beams	66 to 273	0.180	0.005

5. Example of 13-story building

In order to show the possible applications and potential of the proposed methodology to real world structures, a more complex structure is presented in this example. The 13-story building shown in Fig. 14 is taken under study. This structure was already considered in Ref. [37].

This frame is modeled using a total of 226 nodes and 273 elements and it is composed of a set of 8 different sections described in Fig. 14 and Table 3. Therefore, the size of the system of equations is 678×678. In this study, all these 16 mechanical parameters are perturbed by random numbers in order to simulate measurement errors. To illustrate the robustness
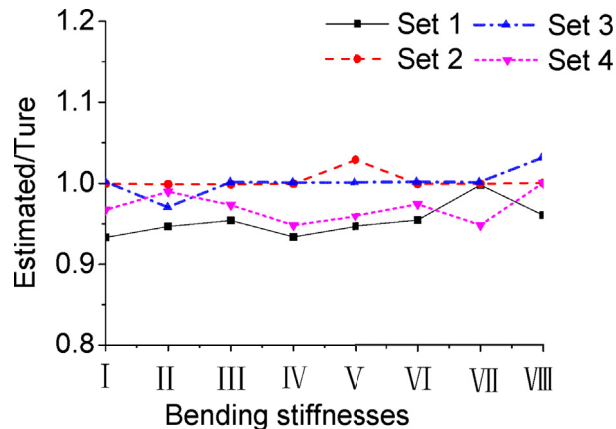

Fig. 15. Estimated bending stiffnesses in four random perturbation factors sets.

of the dynamic COM, four sets of the 16 mechanical parameters are synthesized by the product of the intact values and random numbers evenly distributed in the interval [0.8, 1.2], referred as perturbation factors later. The first mode shape of this frame calculated by SAP200 using these four parameter sets and shown in Fig. 14c) is used as the input of dynamic SSI by COM.

Performing a global study is of interest whenever it might be necessary to know the state of the whole structure or when the damage location is unknown. One study is carried out in order to check the effectiveness of the method, considering a set of known measurements. These sets of known measurements are measured at nodes 5, 9, 14, 19, 23, 28, 33, 37, 42, 47, 51, 56, 61, 65, 70 consisting on the vertical and horizontal displacements in the first mode at each of the mentioned nodes as seen in Fig. 14 (b) and 14 (c). The unknown parameters are bending stiffness, *EI* of elements I to VIII and the displacements of the nodes that are not measured. The areas of elements are assumed to take the theoretical values. For this purpose, the estimated values of the structural parameters in four different sets affected by random perturbed factors of mechanical parameters are provided in Fig. 15. The values of flexural stiffness are bounded as they have a physical meaning; their values cannot be neither negative or extremely high. Hence, the range for estimated normalized values should be in the range [0, 1.5]. From the observed ratio between the estimate and the true value, the error is within 8%, which is acceptable. It should be noted that no inertia (bending stiffness) can be identified by OM, while all these parameters are yielded by COM using only the first-mode information.

6. Conclusions

This article proposes the first application of constrained observability techniques for parametric estimation of structures using dynamic information such as frequencies and mode-shapes.

The nonlinearity of the system obtained when observability is applied, can be properly treated to identify the unknown variables by rearranging the matrix expression and moving the parameters to the modified vectors of mode-shapes and by considering the coupled variables as single variables. After that, the nonlinear constraints between the unknowns are added to tackle the issue of partial observability, as can be seen in Section 4.1 and the example in Section 4.2. Besides, the merit of the dynamic COM is demonstrated as a good solution to the fully observability which OM cannot achieve. In order to verify the feasibility of this method, two examples using experimental data are used as a proof of concept. In both examples, the dynamic COM shows acceptable errors of frequencies and MAC, providing similar or sometimes higher accuracy compared to the reference data. The identified frequencies are approved with less than 2% error with respect to the experimental ones. At the same time, the errors in the MAC values are less than 3% in the first example and 0.5% in the second example. However, a main advantage is obtained by using dynamic COM compared to other SSI methods. This is the possibility to identify if a set of available measurements is sufficient or not to uniquely estimate the state of the structure or a part of it.

To test the performance of the proposed method in real world scenarios, a large structure is used whose real mechanical parameters are perturbed by random numbers in order to simulate measurement errors. It can be seen that the flexural stiffness of all elements can be estimated within acceptable errors. These may allow global application and local identification by choosing the most adequate sets of measurements according to the supposed particular condition of the structure. Undergoing researches focus on efficiently dealing with feasible experimental errors in the measurements.

Declaration of competing interests

The authors declare that they have no known competing financial interests or personal relationships that could have appeared to influence the work reported in this paper.

CRediT authorship contribution statement

T. Peng: Formal analysis, Software, Writing - original draft, Validation. **M. Nogal:** Supervision, Writing - review & editing. **J.R. Casas:** Conceptualization, Supervision, Validation. **J.A. Lozano-Galant:** Methodology, Resources. **J. Turmo:** Funding acquisition, Project administration, Supervision.

Acknowledgements

Appendix: List of symbols and notation

Symbol Significance

$\mathbf{B}$	Total coefficient matrix
$\mathbf{B}_i$	Coefficient matrix of ith mode
$\mathbf{B}_{om}$	Coefficient matrix from the last recursive step by OM
$\mathbf{D}$	Total constant vector
$\mathbf{D}_i$	Constant vector of ith mode
$\mathbf{D}_{om}$	Constant vector from the last recursive step by OM
EA_j	Axial stiffness of jth element
EI_j	Flexural stiffness of jth element
$\mathbf{f}$	Vector of forces
$\mathbf{K}$	Stiffness matrix
$\mathbf{K}^*$	Modified stiffness matrices of static analysis
$[\mathbf{K}_i^*]$	Modified stiffness matrices of ith mode
L_j	length of jth element
m_j	Mass density of jth element
$\mathbf{M}$	Mass matrix
$\mathbf{M}_i^*$	Modified mass matrices of ith mode
N_B	Number of boundary condition
N_N	Number of nodes
$[V]$	Null space of $\mathbf{B}$
R	Total number of modes considered
u_{ik}	Horizontal displacement of kth point and i^{th} mode
v_{ik}	Vertical displacement of kth point and i^{th} mode
w_{ik}	Rotation of kth point under i^{th} mode
W_λ	Weight factors of squared frequencies
$W_\varnothing$	Weight factors of mode-shapes
$\mathbf{z}$	Total vector of unknowns
$\mathbf{z}_i$	Vector of unknowns of ith mode
$\mathbf{z}_{nh}$	Vector of homogeneous solution
$\mathbf{z}_{om}$	Vector of unknowns from the last recursive step by OM
$\mathbf{z}_p$	Particular solution
$\boldsymbol{\delta}$	Vector of displacements
$\boldsymbol{\delta}^*$	Vector of knowns and unknowns of static analysis
ε	Squared sum of the residual
$\varnothing_i$	Mode-shape vector under i^{th} mode
$\varnothing_{mi}$	Measured mode-shape vector under i^{th} mode
$\widetilde{\varnothing_{mi}}$	Estimated mode-shape vector under i^{th} mode corresponded to measured nodes
$\varnothing_{Ki}^*$	Modified modal shapes for the part of stiffness and i^{th} mode
$\varnothing_{Mi}^*$	Modified modal shapes for the part of mass and i^{th} mode
λ_i	Theoretical circular frequency under i^{th} mode
$\widetilde{\lambda}_i$	Measured frequencies, $\widetilde{\lambda}$
$\Delta\lambda_i$	Differences between the measured, $\widetilde{\lambda}_i$, and the estimated frequencies

References

[1] E. Castillo, J.A. Lozano-Galant, M. Nogal, J. Turmo, New tool to help decision making in civil engineering, J. Civ. Eng. Manag. 21 (2015) 689–697, https://doi.org/10.3846/13923730.2014.893904.

[2] M. Pimentel, J. Figueiras, Assessment of an existing fully prestressed box-girder bridge, Proc. Inst. Civ. Eng. Bridg. Eng. 170 (1) (2017) 1–12, https://doi.org/10.1680/jbren.15.00014.

[3] H. B Xiong, J.X. Cao, F.L. Zhang, Xiang, Investigation of the SHM-oriented model and dynamic characteristics of a super-tall building, Smart Struct. Syst. 23 (3) (2019) 295–306, https://doi.org/10.12989/sss.2019.23.3.295.

[4] E.C. Bentz, N.A. Hoult, Bridge model updating using distributed sensor data, Proc. Inst. Civ. Eng. - Bridg. Eng. 170 (1) (2017) 74–86, https://doi.org/10.1680/jbren.15.00030.

[5] J.-N. Juang, M. Phan, Linear system identification via backward-time observer models, J. Guid. Contr. Dynam. 17 (1994) 505–512, https://doi.org/10.2514/3.21227.

[6] S. Li, E. Reynders, K. Maes, G. De Roeck, Vibration-based estimation of axial force for a beam member with uncertain boundary conditions, J. Sound Vib. 332 (2013) 795–806, https://doi.org/10.1016/j.jsv.2012.10.019.

[7] K. Maes, J. Peeters, E. Reynders, G. Lombaert, G. De Roeck, Identification of axial forces in beam members by local vibration measurements, J. Sound Vib. 332 (2013) 5417–5432, https://doi.org/10.1016/j.jsv.2013.05.017.

[8] O. Abdeljaber, O. Avci, S. Kiranyaz, M. Gabbouj, D.J. Inman, Real-time vibration-based structural damage detection using one-dimensional convolutional neural networks, J. Sound Vib. 388 (2017) 154–170, https://doi.org/10.1016/j.jsv.2016.10.043.

[9] J.X. Cao, H.B. Xiong, J.W. Chen, Alexandre Huynh, Bayesian parameter identification for empirical model of CLT connections, Construct. Build. Mater. 218 (2019) 254–269, https://doi.org/10.1016/j.conbuildmat.2019.05.051.

[10] S.G. Torres Cedillo, P. Bonello, An equivalent unbalance identification method for the balancing of nonlinear squeeze-film damped rotordynamic systems, J. Sound Vib. 360 (2016) 53–73, https://doi.org/10.1016/j.jsv.2015.08.028.

[11] M.D. Spiridonakos, S.D. Fassois, Parametric identification of a time-varying structure based on vector vibration response measurements, Mech. Syst. Signal Process. 23 (2009) 2029–2048, https://doi.org/10.1016/j.ymssp.2008.11.004.

[12] E. Viola, P. Bocchini, Non-destructive parametric system identification and damage detection in truss structures by static tests, Struct. Infrastruct. Eng. 9 (2013) 384–402, https://doi.org/10.1080/15732479.2011.560164.

[13] P. Hajela, F.J. Soeiro, Structural damage detection based on static and modal analysis, AIAA J. 28 (1990) 1110–1115, https://doi.org/10.2514/3.25174.

[14] K.D. Hjelmstad, S. Shin, Damage detection and assessment of structures from static response, J. Eng. Mech. 123 (1997) 568–576, https://doi.org/10.1061/(ASCE)0733-9399(1997)123:6(568).

[15] T. Kijewski, A. Kareem, Wavelet transforms for system identification in civil engineering, Comput. Civ. Infrastruct. Eng. 18 (2003) 339–355, https://doi.org/10.1111/1467-8667.t01-1-00312.

[16] C.S. Huang, S.L. Hung, C.I. Lin, W.C. Su, A wavelet-based approach to identifying structural modal parameters from seismic response and free vibration data, Comput. Civ. Infrastruct. Eng. 20 (2005) 408–423, https://doi.org/10.1111/j.1467-8667.2005.00406.x.

[17] R. Tarinejad, M. Damadipour, Modal identification of structures by a novel approach based on FDD-wavelet method, J. Sound Vib. 333 (2014) 1024–1045, https://doi.org/10.1016/j.jsv.2013.09.038.

[18] Z. Zhou, H. Adeli, Time-frequency signal analysis of earthquake records using Mexican hat wavelets, Comput. Civ. Infrastruct. Eng. 18 (2003) 379–389, https://doi.org/10.1111/1467-8667.t01-1-00315.

[19] R. Perera, R. Marin, A. Ruiz, Static-dynamic multi-scale structural damage identification in a multi-objective framework, J. Sound Vib. 332 (2013) 1484–1500, https://doi.org/10.1016/j.jsv.2012.10.033.

[20] M. Sanayei, B. Arya, E.M. Santini, S. Wadia-Fascetti, Significance of modeling error in structural parameter estimation, Comput. Civ. Infrastruct. Eng. 16 (2001) 12–27, https://doi.org/10.1111/0885-9507.00210.

[21] S. Díaz, J. González, R. Mínguez, Observability analysis in water transport networks: algebraic approach, J. Water Resour. Plann. Manag. 142 (2016), https://doi.org/10.1061/(ASCE)WR.1943-5452.0000621.

[22] E. Castillo, A.J. Conejo, R. Eva Pruneda, C. Solares, Observability in linear systems of equations and inequalities: applications, Comput, Oper. Res. 34 (2007) 1708–1720, https://doi.org/10.1016/j.cor.2005.05.035.

[23] E. Castillo, A.J. Conejo, R.E. Pruneda, C. Solares, Observability analysis in state estimation: a unified numerical approach, IEEE Trans. Power Syst. 21 (2006) 877–886, https://doi.org/10.1109/TPWRS.2006.873418.

[24] E. Castillo, A.J. Conejo, J.M. Menéndez, P. Jiménez, The observability problem in traffic network models, Comput. Civ. Infrastruct. Eng. 23 (2008) 208–222, https://doi.org/10.1111/j.1467-8667.2008.00531.x.

[25] E. Castillo, M. Nogal, A. Rivas, S. Sánchez-Cambronero, Observability of traffic networks. Optimal location of counting and scanning devices, Transport. Bus.: Transport Dynamics 1 (1) (2013) 68–102, https://doi.org/10.1080/21680566.2013.780987.

[26] J. Lei, M. Nogal, J.A. Lozano-Galant, D. Xu, J. Turmo, Constrained observability method in static structural system identification, Struct. Contr. Health Monit. 25.1 (2018), e2040, https://doi.org/10.1002/stc.2040.

[27] K.D. Hjelmstad, M.R. Banan, M.R. Banan, On building finite element models of structures from modal response, Earthq. Eng. Struct. Dynam. 24 (1995) 53–67, https://doi.org/10.1002/eqe.4290240105.

[28] J.A. Lozano-Galant, M. Nogal, E. Castillo, J. Turmo, Application of observability techniques to structural system identification, Comput. Civ. Infrastruct. Eng. 28 (2013) 434–450, https://doi.org/10.1111/mice.12004.

[29] I. JOSA, Dynamic Structural System Identification, Master Thesis, Universidad Politécnica de Catalunya, 2017.

[30] Y. Haralampidis, C. Papadimitriou, M. Pavlidou, Multi-objective framework for structural model identification, Earthq. Eng. Struct. Dynam. 34 (2010) 665–685, https://doi.org/10.1002/eqe.449.

[31] H.F. Lam, Structural Model Updating and Health Monitoring in the Presence of Modeling Uncertainties, ph.D thesis, Department of Civil Engineering, Hong Kong University of Science and Technology, Hong Kong, 1998.

[32] E. Simoen, G.D. Roeck, G. Lombaert, Dealing with uncertainty in model updating for damage assessment:a review, Mech. Syst. Signal Process. 56 (2015) 123–149, https://doi.org/10.1016/j.ymssp.2014.11.001.

[33] G. Murat, A. Suleyman, C.A. Ahmet, Experimental investigation on acceptable difference value in modal parameters for model updating using RC building models, Struct. Eng. Int. 8 (2018) 1–10, https://doi.org/10.1080/10168664.2018.1517019.

[34] J.A. Lozano-Galant, M. Nogal, J. Turmo, E. Castillo, Selection of measurement sets in static structural identification of bridges using observability trees, Comput. Concr. 15 (2015) 771–794, https://doi.org/10.12989/cac.2015.15.5.771.

[35] M. Nogal, J.A. Lozano-Galant, J. Turmo, E. Castillo, Numerical damage identification of structures by observability techniques based on static loading tests, Struct. Infrastruct. Eng. 12 (2016) 1216–1227, https://doi.org/10.1080/15732479.2015.1101143.

[36] J. Lei, J.A. Lozano-Galant, M. Nogal, D. Xu, J. Turmo, Analysis of measurement and simulation errors in structural system identification by observability techniques, Struct. Contr. Health Monit. 24 (2017) 6, https://doi.org/10.1002/stc.1923.

[37] J. Lei, D. Xu, J. Turmo, Static structural system identification for beam-like structures using compatibility conditions, Struct. Contr. Health Monit. 25 (2018), e2062, https://doi.org/10.1002/stc.2062.

[38] J.A. Lozano-Galant, M. Nogal, I. Paya-Zaforteza, J. Turmo, Structural system identification of cable-stayed bridges with observability techniques, Struct. Infrastruct. Eng. 10 (2014) 1331–1344, https://doi.org/10.1080/15732479.2013.807292.

[39] A. Boris Zárate, J.M. Caicedo, Finite element model updating: multiple alternatives, Eng. Struct. 30 (12) (2008) 3724–3730, https://doi.org/10.1016/j.engstruct.2008.06.012.